JOURNAL OF MATERIALS SCIENCE 29 (1994) 3151–3160

Effects of distortional components in biaxial stretching of poly(ethylene terephthalate) sheets on dimensional stability and structure

L. MASCIA, Z. FEKKAI
Institute of Polymer Technology and Materials Engineering, Loughborough University of Technology, Loughborough, Leics LE11 3TU, UK

G. GUERRA, L. PARRAVICINI, F. AURIEMMA
Dipartimento di Chimica, Universita' di Napoli – Federico II, Via Mezzocannone 4, I-80134 Naples, Italy

Thin sheets of poly(ethylene terephthalate) were stretched biaxially over a wide range to temperatures below the melting point of the polymer. The linear shrinkage occurring at temperatures between 85 and 100 °C decreased with increasing draw temperature and draw ratio. Specimens taken near the edges of the drawn sheets, which had been subjected to in-plane shear deformations, were found to exhibit linear shrinkage 5–8 times lower than those taken from the middle of the sheet. Subsequent experiments, using purpose-built clamps to achieve a more uniform state of shear in both directions of the biaxially drawn samples, confirmed the universality of the principle of shrinkage suppression by the superposition of shear deformations. X-ray diffraction studies revealed that the phenomenon was not related to differences in type of orientation of the crystals. The information from the X-ray diffraction studies and data from thermal analysis have led to the conclusion that the enhanced dimensional stability of biaxially drawn sheets subjected to superimposed shear deformations results from a combination of a higher rate of stress-induced crystallization and a reduction in the level of orientation within the amorphous phase.

1. Introduction

The possibility of inducing orientation of amorphous and crystalline domains by biaxial stretching operations is the predominant factor responsible for the development of polyethylene terephthalate (PET) films and bottles [1–4]. Alongside the industrial developments over the last 40 years or so concerned with the efficiency of biaxial drawing operations, there have been extensive studies aimed at elucidating the influence of process variables on properties [5–15].

The mechanism associated with the alignment of crystallites and molecules in the biaxial stretching of PET products is unique in so far as the polymer has initially a rather low level of crystallinity and, therefore, crystallization and orientation phenomena take place simultaneously during the drawing process. Since such a mechanism precludes the necessity of having to break down any spherulitic entities present within the material, there are fewer constraints to the alignment of crystals during drawing and, as a consequence, lower levels of internal stresses are set up in the final products. This results in a high degree of dimensional stability at ambient temperatures but, since the polymer may not reach its maximum level of crystallinity during drawing, further crystallization can occur when it is subsequently heated above its T_g. Added to the molecular motions associated with relaxation of orientation, this may cause large retractions along the drawing directions [16–20].

In work reported elsewhere [16] it was shown that linear retraction at temperatures above 85 °C of samples drawn monoaxially, under different conditions, is directly proportional to the heat of crystallization, which extrapolates to zero for samples that are dimensionally stable. Accordingly the heat of fusion was found to increase for samples exhibiting lower shrinkage, reaching a maximum corresponding to the value obtained for samples which were dimensionally stable, such as those that were annealed under constraints at temperatures sufficiently high to promote rapid thermal crystallization.

In the production of films and fibres dimensional stability is induced, in fact, through annealing operations and is facilitated by allowing a small amount of retraction to take place. In the production of bottles, on the other hand, there are major engineering restrictions in performing in-line annealing operations. Consequently shrinkage remains a major problem for applications where bottles are exposed to high temperatures, such as in sterilization and filling with hot liquids.

To this end a study was carried out to examine stress-induced crystallization phenomena resulting from the superimposition of in-plane shear deforma-

0022–2461

tions in the stretching of PET sheets. This state of deformation could be adopted in a bottle blowing process whereby a torsion would be added to the axial stretching operation carried out on the preforms, prior to or during the pressurization stage of the expansion process.

2. Experimental procedure

Sheets of PET 0.8 mm thick, produced by extrusion using a high molecular weight polymer grade (Intrinsic Viscosity (IV) = 0.8), were cut into 50 mm × 50 mm square sections. On one surface were scribed grids 5 mm square (Fig. 1a), and a variety of slits were cut out at the corners to produce different gripping geometries.

A specially constructed biaxial stretching device was fixed to a tensile testing apparatus, fitted with an environmental chamber heated by recirculated hot air. As the clamps of the stretching jig were only capable of extending to twice the original distance between clamps along both axes, larger draw ratios were achieved by cutting out specimens in the shape of a Maltese cross with the gripping area extended to the central section (Fig. 2a). With the specimens shown in Figs 1a and 2a the central regions could be drawn to 2:1 and 3.5:1, respectively, in both axial directions (Figs 1b and 2b). These diagrams show that the corner sections of the drawn samples assume a rhomboidal geometry, which is indicative of a stretching process comprising a combination of extension and in-plane shear deformations. In other words, while the central sections are subjected to pure biaxial drawing which is described by two axial draw ratios λ_x^T and λ_y^T (where $\lambda_x^T = \lambda_y^T$), the stretched state of the corner sections has to be described by the above axial draw ratios and two additional shear ratios λ_{xy}^S and λ_{yx}^S (see Appendix).

In order to widen the range of combinations of biaxial stretching with shear, specimens were cut out to the geometry in Fig. 3a so that the axial movements of the clamps along the two perpendicular directions would compel the central regions of the specimens to undergo biaxial stretching and in-plane shear deformations, as shown in Fig. 3b. The angle formed by the slits with the direction of movement of the clamps had to be carefully selected to prevent the central regions undergoing simple rotations and subsequently causing monoaxial drawing, thus preventing the central

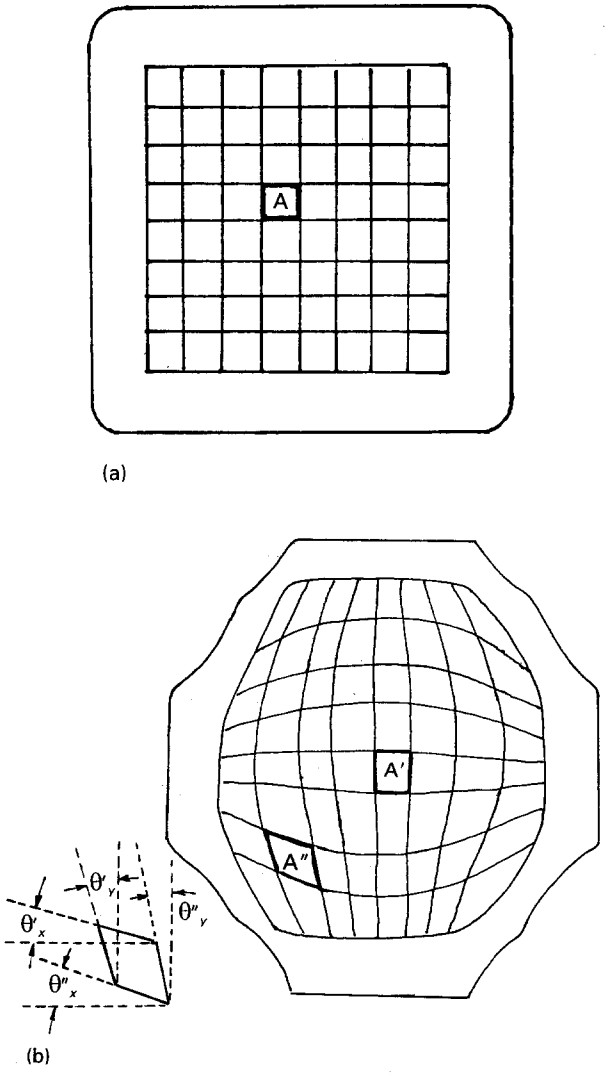

Figure 1 Geometry of samples used in balanced biaxial stretching experiments to low draw ratio (DR = 2.0:1): (a) sample (square) before stretching, (b) sample (octohedral) after stretching, showing shear deformations and angles of distortion in the corner regions.

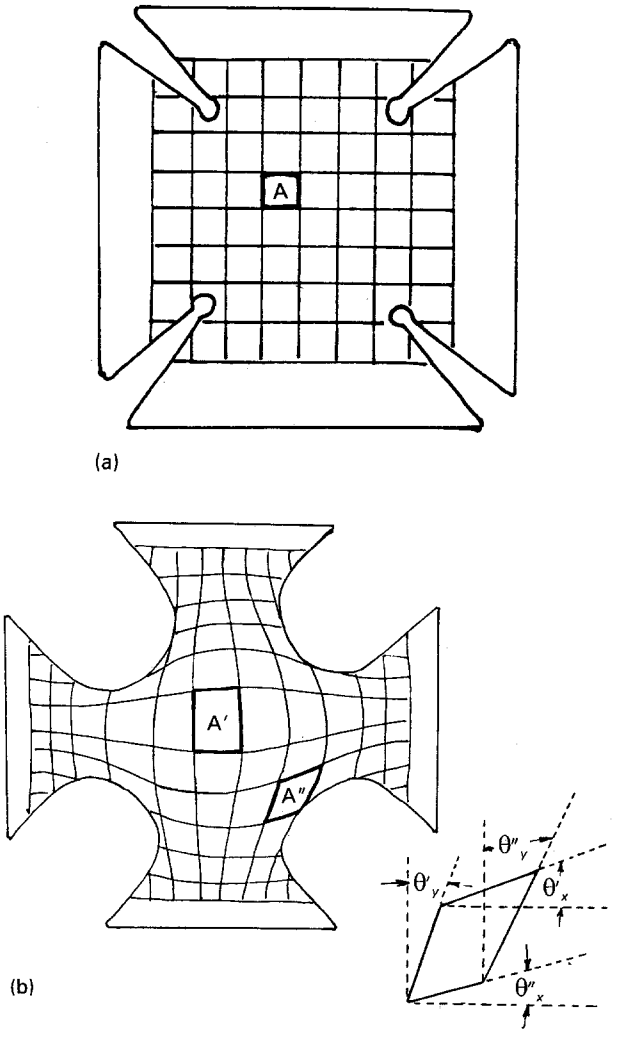

Figure 2 Geometry of samples used in balanced biaxial stretching experiments to high draw ratio (DR = 3.5:1): (a) sample (Maltese cross) before stretching, (b) sample after stretching, showing shear deformations and angles of distortion in the corner regions.

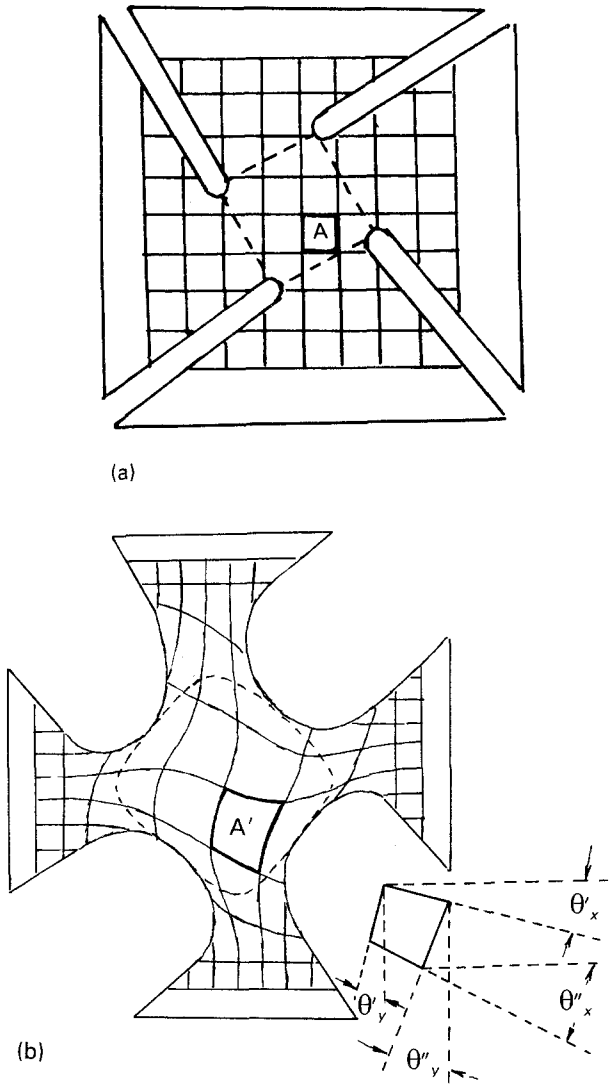

Figure 3 Geometry of samples used in equally biaxially stretching experiments with superimposed in-plane distortions: (a) sample before stretching, (b) sample after stretching, showing shear deformations and angles of distortion in the central regions.

regions from being stretched to the intended draw ratio. Difficulties were also experienced with the in-plane shear stretching experiments with respect to slippage at the clamps, giving rise to appreciable variations.

In addition to the above, a limited number of biaxial stretching experiments were also carried out using the Maltese cross specimens gripped in the two perpendicular directions by clamps that protruded by different amounts so that a rectangular, rather than a square, area would be stretched to equal final distances in the two perpendicular directions, thereby giving rise to a state of unbalanced biaxial stretching along the two drawing directions, respectively 3.5:1 and 2.0:1.

In all cases the specimens were drawn over the temperature range 80–125 °C, i.e. above the T_g of the polymer but below the temperature at which appreciable thermal crystallization would occur during the preheating stage, which was kept constant at 3 min. The clamp separation speed was fixed at 200 mm min^{-1} and the samples were immediately quenched with a wet cloth before being removed from the stretching jig. Photographs of the samples being drawn in the biaxial stretching device described earlier, representing two typical situations, are shown in Fig. 4.

Approximately 20 mm square specimens were cut out from the appropriate regions of the drawn samples to calculate the respective axial draw ratios and shear ratios according to the definitions given in the Appendix. These specimens were then immersed in water either at 85 °C or under boiling conditions for 1 min, and their area as well as the shear angles, where applicable, were measured using a fine-grid paper stencil from which the average linear shrinkage was calculated accordingly. In all cases the changes in shear angles caused by shrinkage of the samples were too small to be measured with any degree of accuracy and, therefore, were not taken into account in the calculations.

Differential scanning calorimetry (DSC) was carried out on the drawn samples using a Du Pont 2000 instrument at a heating rate of 20 °C min^{-1} and under a constant flow of nitrogen. The percentage of total crystallinity was calculated using the value of 32.5 cal g^{-1} (135.8 J g^{-1}) for a nominal 100% crystallinity while the degree (%) of stress-induced crystallinity was calculated as follows:

$$A = \% \text{ crystallinity (thermal)}$$

$$= \frac{\Delta H_f(u) - \Delta H_c(u)}{\Delta H_f(100)} \times 100$$

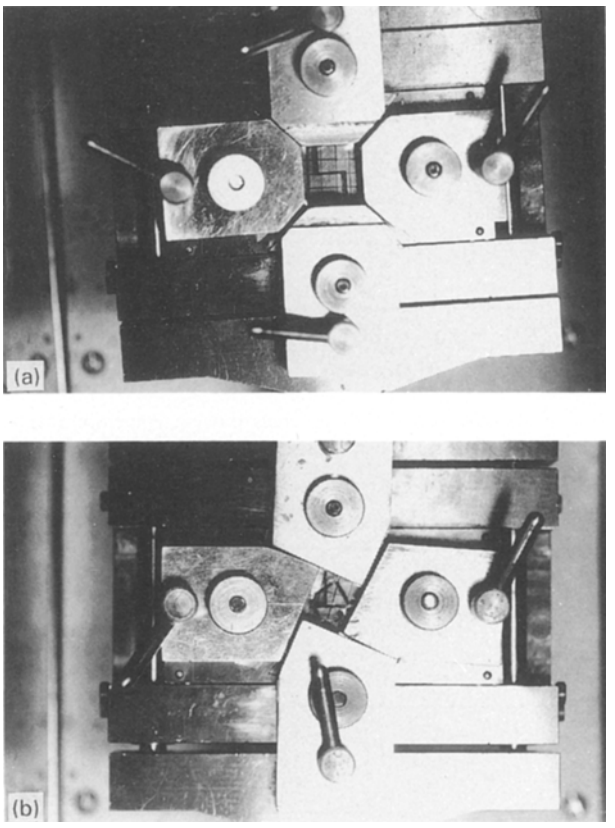

Figure 4 Biaxial stretching jig fitted to a tensile testing machine: (a) balanced biaxial stretching clamps, (b) biaxial stretching clamps with superimposed in-plane distortions.

$$B = \%\ \text{crystallinity (thermal + stress-induced)} = \frac{\Delta H_f(o) - \Delta H_c(o)}{\Delta H_f(100)} \times 100$$

Therefore

$$C = \%\ \text{stress-induced crystallinity} = B - A = \frac{\Delta H_f(o) - \Delta H_f(u) - [\Delta H_c(o) - [\Delta H_c(u)]}{\Delta H_f(100)} \times 100$$

where ΔH_c = heat of crystallization in the temperature-rise scan, ΔH_f = overall heat of fusion, $\Delta H_f(100)$ = heat of fusion at 100% crystallinity, (o) = oriented and (u) = unoriented.

The drawn samples were characterized also by X-ray diffraction using a flat camera with Ni-filtered CuK_α radiation. The X-ray diffraction patterns were taken with the beam parallel and perpendicular to the film surface. For diffraction with the beam parallel to the film surface, strips of PET film were cut parallel and perpendicular to the sides of the drawn sections. For identification purposes the three measurement directions are designated as "through", "edge" and "end", respectively [27].

3. Results and discussion

Plots of percentage linear shrinkage against drawing temperature for the central regions of samples biaxially drawn to equal draw ratios in two perpendicular directions are shown in Fig. 5 and in Table I. Both sets of data reveal that linear shrinkage decreases with drawing temperature and with increasing draw ratio.

DSC traces of the samples biaxially drawn to DR = 3.5:1 at various temperatures are shown in Fig. 6. In addition to the glass transition in the temperature range 65–75 °C and the melting endotherm at 250–255 °C, the thermograms for the samples drawn at temperatures below 100 °C show a shallow exothermic peak, whose maximum shifts to higher temperatures with increasing drawing temperature. An analogous behaviour has been observed for uniaxially drawn films and fibres [16, 21–26]. Similar broad exothermic peaks have been associated with crystallization phenomena of PET in its mesomorphic phase [26].

The DSC traces for samples drawn at higher temperatures (110 and 125 °C), on the other hand, are similar to those obtained for the unstretched film (Fig. 6). This suggests that the drawing operation at these higher temperatures produces low levels of crystallinity. A similar behaviour was observed for samples drawn biaxially to DR = 2:1 (Fig. 7, curves a_1 and a_2). In this case sharp exothermic peaks are experienced even at lower drawing temperatures, i.e. 80 and 90 °C, indicating that a lower extent of stress-induced crystallization has taken place during drawing (see also DSC data in Table II).

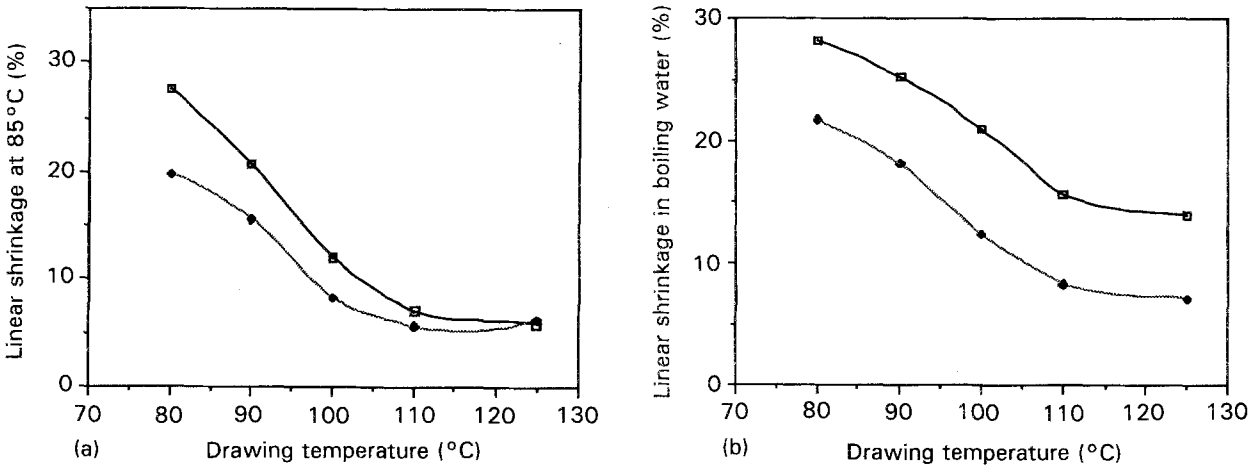

Figure 5 Plots of linear shrinkage versus drawing temperature for balanced biaxially stretched samples at two draw ratios: (□) 2:1, (◆) 3.5:1. (a) Shrinkage at 85 °C, (b) shrinkage at 100 °C.

TABLE I Average linear shrinkage in water at 100 °C for various representative samples

Drawing temperature (°C)	Shrinkage (%) Balanced biaxial stretching[a]		Unbalanced biaxial stretching ($\lambda_W = 2.0$, $\lambda_L = 3.5$)[b]	Shear regions of balanced biaxially stretched samples ($\lambda_T = 1.67$, $\lambda_S = 1.16$)[c]	Central regions of samples biaxially stretched with superimposed in-plane shear ($\lambda_T = 1.80$, $\lambda_S = 1.14$)[c]
	$\bar{\lambda} = 2.0$	$\bar{\lambda} = 3.5$			
90	25.1	18.2	20.4	4.8	5.7
100	21.0	12.6	10.3	3.6	3.4
110	16.2	8.5	7.8	1.8	2.0

[a] $\bar{\lambda}$ = Average axial draw ratio.
[b] λ_W = Draw ratio in the width direction, λ_L = draw ratio in the length direction.
[c] λ_T = Average extensional draw ratio in the two principal directions; λ_S = average shear ratio, calculated from the average angle of distortion from the two drawing directions.

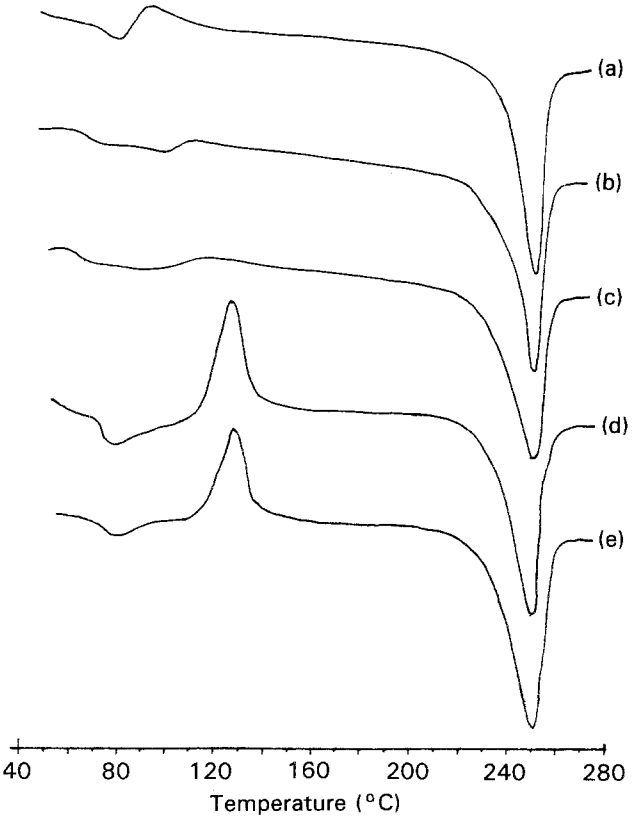

Figure 6 DSC thermograms at 20 °C min^{-1} heating rate of samples taken from the middle of sheets, balanced biaxially drawn to 3.5:1 at different drawing temperatures: (a) 80 °C, (b) 90 °C, (c) 100 °C, (d) 110 °C, (e) 125 °C.

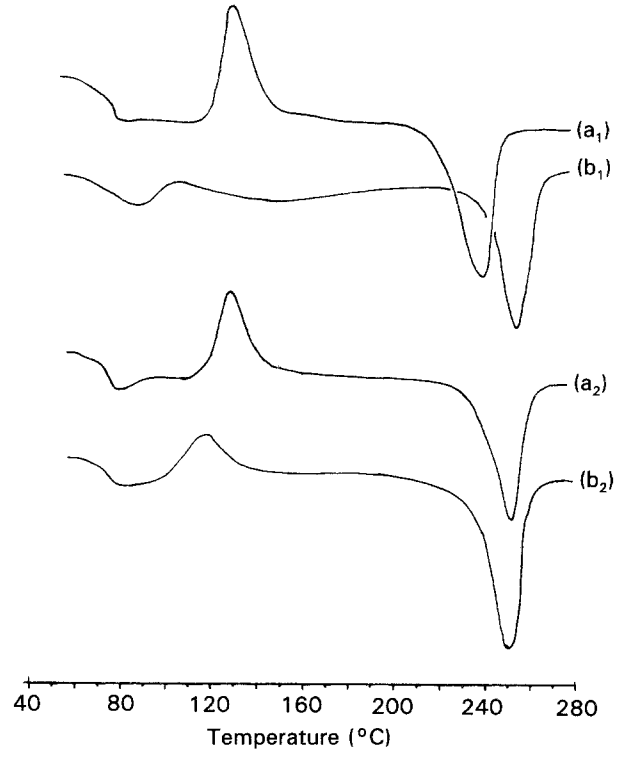

Figure 7 DSC thermograms at 20 °C min^{-1} heating rate of samples balanced biaxially drawn to 2.0:1. (a) Specimens taken from the middle region, (b) specimens taken from the shear region; (a_1, b_1) drawn at 80 °C, (a_2, b_2) drawn at 90 °C.

The X-ray diffraction patterns for samples taken from the central regions of sheets subjected to a biaxial draw ratio of 3.5:1 at a drawing temperature of 90 °C are reported in Fig. 8. Fig. 8a was obtained with the X-ray beam perpendicular to the film surface ("through" direction), while Figs 8b and c were obtained with the X-ray beam parallel to the film surface ("edge" and "end", respectively).

Beside some diffuse scattering rings, the X-ray diffraction pattern for the "through" direction displays an intense and nearly complete ring corresponding to the (0 1 0) reflection of the triclinic structure of PET [28, 29] (Fig. 8a). The two corresponding patterns obtained along the "edge" and "end" directions are similar to each other, and display the reflections (1 0 0) and (−1 1 0) on the equator and the (0 1 0) reflection on the meridian (Fig. 8b and c). This indicates the existence of a type of orientation close to what is known as "uniplanar" [30, 31], where the crystal plane indexed (1 0 0) containing the planes of the aromatic rings tends to assume an orientation parallel to the film surface, while the *c* axes of the crystals assume a random orientation in the plane of the film. A perfect uniplanar structure would present only rings on Fig. 8a, while Figs 8b and c would be identical. The broad diffraction peaks in the patterns in Fig. 8, on the other hand, are indicative of a paracrystalline order with the crystalline phase.

By increasing the drawing temperature from 90 to 100 °C, the "uniplanar" orientation is maintained but there is a marked decrease in both level of orientation and degree of crystallinity. A further increase in drawing temperature up to 110 °C produces an essentially amorphous and unoriented morphology, which is confirmed by the occurrence of a strong exotherm in the DSC scan (Fig. 6d).

By examining together the DSC data (Figs 6 and 7) and the results of the X-ray diffraction analysis (Fig. 8) it is possible to provide an interpretation for the shrinkage behaviour of biaxially drawn samples, as illustrated in Fig. 5, from considerations regarding the levels of orientation and crystallinity. For such a purpose it is reasonable to assume that the decrease in linear shrinkage experienced by increasing the drawing temperature (shown in Fig. 5) is mainly related to the corresponding reduction in orientation of the amorphous phase. The higher levels of shrinkage for samples made at a draw ratio DR = 2.0:1, relative to those for the samples drawn at DR = 3.5:1, has to be associated with the wider crystallization phenomena which may occur during shrinkage experiments on the former samples, since these display a fairly high level of orientation in the amorphous phase and a low degree of stress-induced crystallinity (see Table II, column 5).

Chandran and Jabarin [32] have shown that the upturn in the stress–extension ratio curves recorded during biaxial drawing of PET sheets, which is indicative of the onset of stress-induced crystallization, begins to take place at draw ratios just above 3.5 for drawing temperatures around 105 °C, decreasing to lower draw ratios with decreasing temperature and increasing drawing rates. For comparison purposes, note that the drawing rates used in the present study are considerably lower than those used by the above authors.

Plots of linear shrinkage against drawing temperature for some of the samples taken from the shear

TABLE II Typical DSC data biaxially drawn PET samples

	λ^T (X:1)	DT (°C)[a]	ΔH_c (cal g^{-1})[b]	T_c (°C)[c]	ΔH_f (cal g^{-1})[d]	T_m (°C)[e]	Stress-induced crystallinity (%)
Biaxial drawing							
Central regions	2.0	80	5.59	124.9	9.85	248.1	8.6
Shear regions (λ_S = 1.09)	1.4	80	2.13	106.1	10.90	248.1	22.5
Central regions	2.0	100	5.09	125.5	8.68	250.5	6.5
Shear regions (λ_S = 1.09)	1.4	100	2.98	115.2	10.55	249.2	18.8
Biaxial drawing with superimposed planar distortions							
λ_S = 1.14	1.80	80	2.15	96.1	8.74	251.1	15.8
λ_S = 1.14	1.80	100	0.49	116.3	10.58	251.0	26.5

[a] DT = Drawing temperature.
[b] ΔH_c = Heat of crystallization in the temperature-rise scan; 1 cal = 4.19 J.
[c] T_c = Peak exotherm temperature (cold crystallization).
[d] ΔH_f = Overall heat of fusion.
[e] T_m = Peak endotherm temperature (melting).

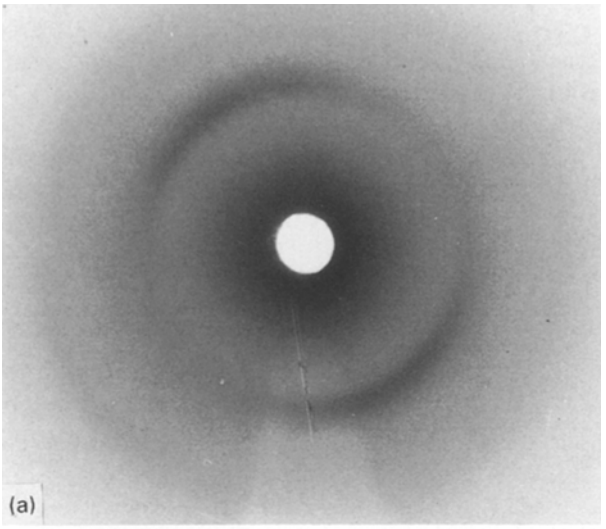

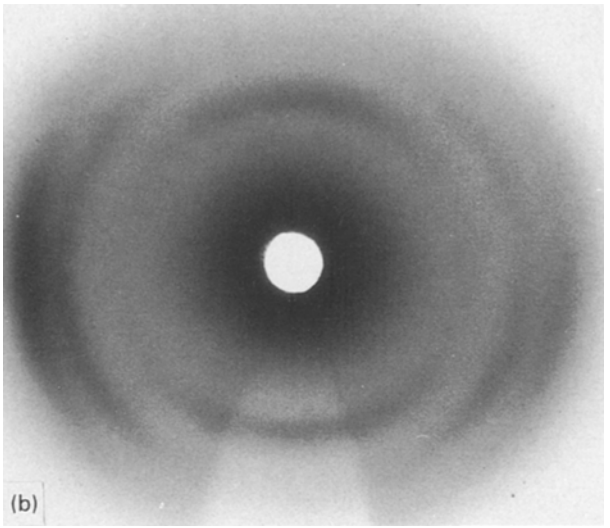

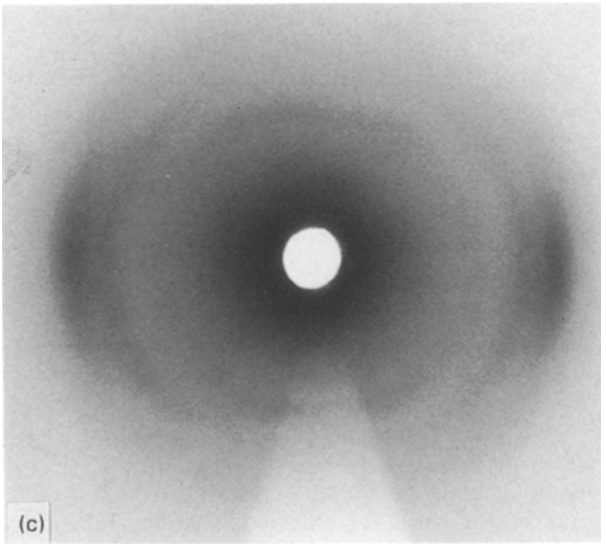

Figure 8 X-ray diffraction patterns for specimens taken from the central region of the sample balanced biaxially drawn to 3.5:1 at 90 °C drawing temperature: directions (a) "through", (b) "edge", (c) "end".

region of the biaxially drawn sheet are shown in Fig. 9 and Table I (column 5), while the results for samples drawn biaxially with superimposed in-plane shear are shown in Table I, column 6. Both sets of data indicate that biaxial stretching with superimposed shear produces a very large reduction in shrinkage. At equal area expansion ratio, in fact, the difference is by a factor of 5 to 8.

Some representative DSC traces for specimens taken from the shear region of samples drawn at DR = 2:1 are shown in Fig. 7 and in Table II. These data clearly show that, even at low draw ratios, the superposition of shear deformation on biaxial stretching has the effect of increasing considerably the degree of crystallinity in the drawn samples through stress-induced crystallization. High degrees of crystallinity were also observed for samples drawn biaxially with a superimposed in-plane shear, which were found to exhibit similar reductions in level of shrinkage.

However, for samples drawn biaxially at 80 and 100 °C to DR = 3.5:1, the specimens taken from the central and in the shear regions, although exhibiting vastly different levels of shrinkage (Figs. 5 and 9) display similar thermal behaviour in DSC scans, i.e. both samples show shallow crystallization exothermic peaks and exhibit a high degree of crystallinity

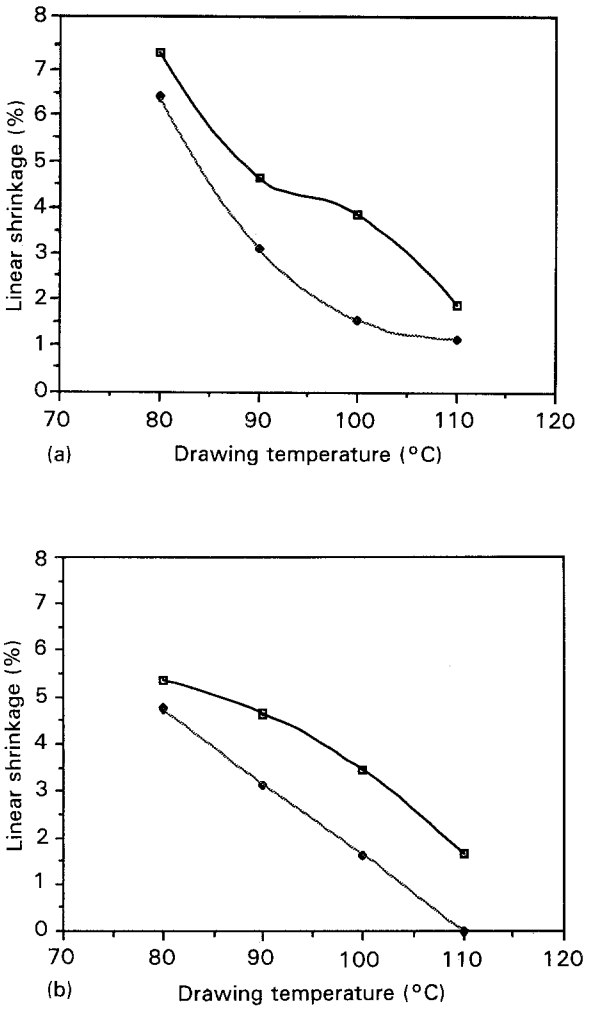

Figure 9 Plots of linear shrinkage at (⊡) 100 °C and (◆) 85 °C versus drawing temperature for specimens taken from the shear (corner) regions of balanced biaxially drawn samples: (a) draw ratio = 2.0:1, (b) draw ratio = 3.5:1.

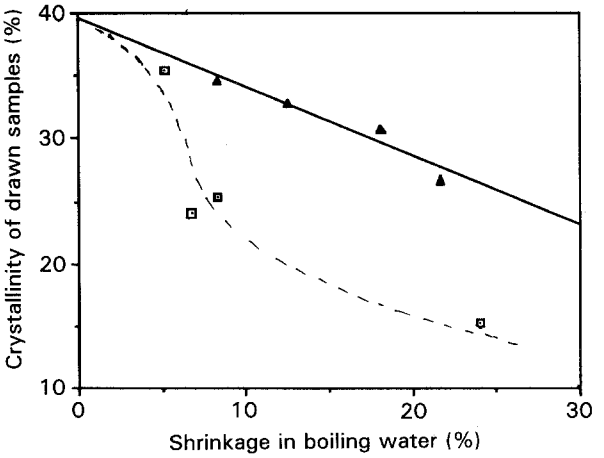

Figure 10 Plots of crystallinity (DSC method) versus linear shrinkage at 100 °C for (⊡) monoaxially drawn samples (DR = 4.0:1) [29] and (▲) balanced biaxially drawn samples, both at various drawing temperatures.

(Table II). Hence the overall level of crystallinity alone cannot account for differences in the shrinkage behaviour of samples experiencing multiaxial stresses during drawing. It is instructive to consider, in this respect, the relationship between overall degree of crystallinity and average linear shrinkage for samples drawn monoaxially at DR = 4:1 and those drawn biaxially at DR = 3.5:1. Fig. 10 shows that there is a clear discrepancy between the two relationships and that, at equal levels of overall crystallinity, biaxially drawn samples can exhibit a substantially lower amount of shrinkage.

The X-ray diffraction patterns for specimens taken from the shear region of the sheet subjected to a biaxial draw ratio of 3.5:1 at a drawing temperature of 90 °C, which were examined with the beam parallel to three mutually perpendicular directions (i.e. "through", "edge" and "end") are shown in Fig. 11a–c, respectively. These samples display a "uniplanar axial" orientation [30, 31], also known as "double orientation" [33, 35]. In particular the *c* axes of the crystals are oriented along the main drawing direction and (as for the PET samples with a "uniplanar" orientation) the crystal planes (1 0 0) tend to be oriented parallel to the film surface. The pattern obtained along the "through" direction shows corresponding intense sharp reflections with (0 1 0) and (0 −1 1) indexes, while for the pattern obtained along the "edge" direction there is an intense and highly oriented halo on the equator, in the region of the (−1 1 0) and (1 0 0) reflections. The pattern along the "end" direction presents only a well-defined sharp reflection in the meridional region, corresponding to the (0 1 0) reflection. It is also worth noting that the broad nature of the reflections in the patterns of Fig. 11 is indicative of the presence of some paracrystallinity, similar to that observed, for instance, in rapidly drawn uniaxially oriented samples [36].

On increasing the drawing temperature from 90 to 110 °C, the "uniplanar axial" orientation and the paracrystallinity of the drawn samples still persist, but there is a marked decrease in the degree of orientation. This is shown, for instance, by a comparison with the patterns obtained for the "through" direction on samples drawn at 90 °C (Fig. 11a), at 100 °C (Fig. 12a) and at 110 °C (Fig. 12b). As for the case of samples taken from the central regions of the sheets, the reduction in the level of shrinkage on increasing the drawing temperature, experienced by samples taken in the shear regions, can be easily accounted for by a corresponding decrease in orientation.

However, the different types of crystalline orientation taking place in the two situations, i.e. uniplanar or uniplanar-axial, respectively, bear no relationship with the shrinkage behaviour of these samples. Furthermore, the samples drawn biaxially with superimposed in-plane shear (Fig. 3), which exhibit a similar very low shrinkage to those taken from the shear regions of the biaxially drawn samples (Fig. 2) exhibit a "uniplanar orientation", i.e. similar to biaxially stretched samples which have not been subjected to in-plane distortions. The geometry of the drawn sections in the middle of the sample is approximately equal to that of a square in both cases, the only difference being a rotation of the sides (in the second case) in relation to the drawing direction. The X-ray diffraction patterns are, in fact, similar to those of

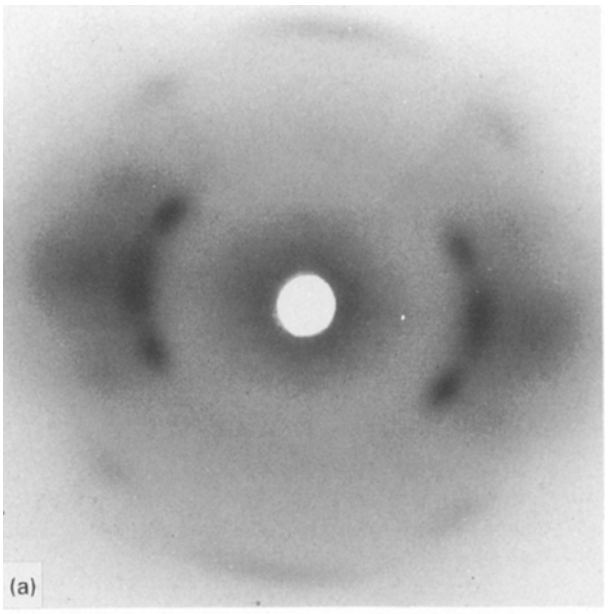

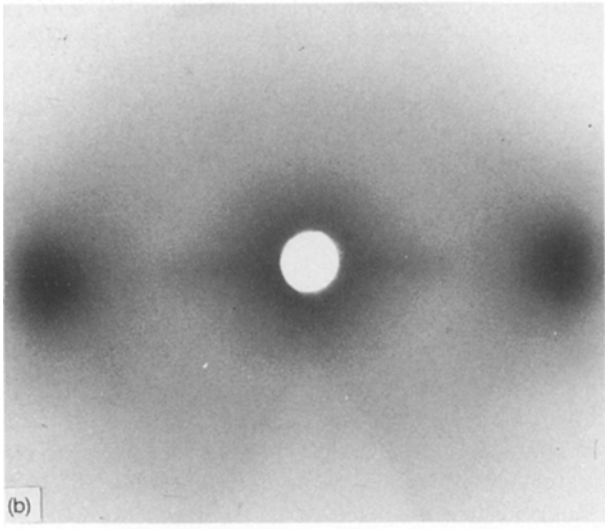

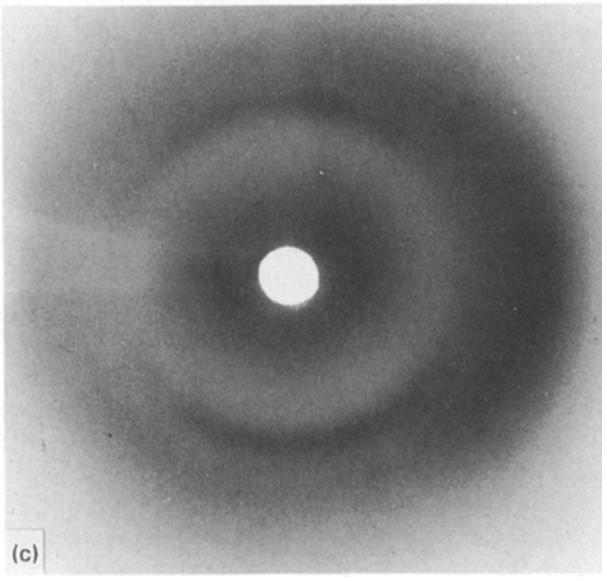

Figure 11 X-ray diffraction patterns to specimens taken from the shear (corner) regions of the samples balanced biaxially drawn to 3.5:1 at 90 °C: directions (a) "through", (b) "edge", (c) "end".

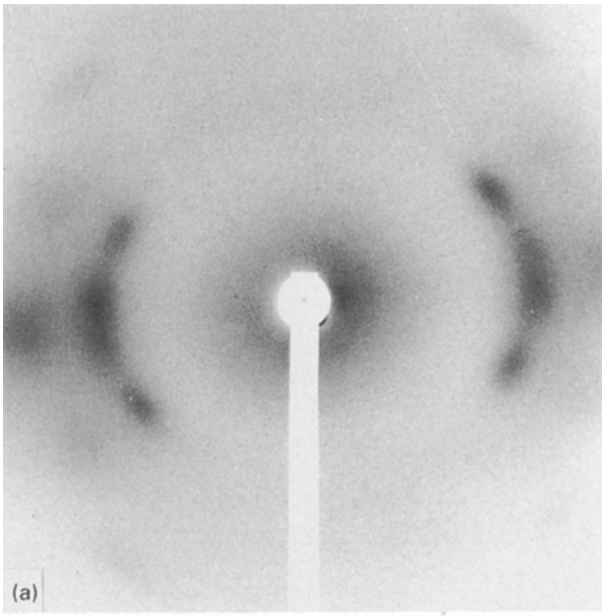

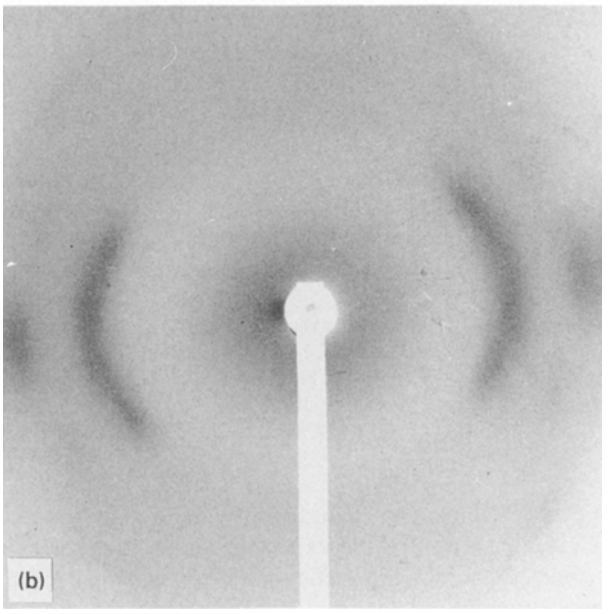

Figure 12 X-ray diffraction patterns ("through" direction) for specimens taken from the shear (corner) regions of balanced biaxially drawn samples to 3.5:1. (a) Drawn at 100 °C, (b) drawn at 110 °C.

Fig. 8 for the central regions of biaxially drawn samples, which exhibit a high level of shrinkage. Consequently, in addition to the degree of crystallinity the type and extent of crystalline orientation have also to be discounted as major causes for the very large reduction in the level of shrinkage brought about by the superposition of shear in the drawing process.

This leads to the conclusion, therefore, that the major factor that determines the shrinkage behaviour has to be the orientation of the amorphous phase. Direct estimates of the extent of orientation of the amorphous phase for the samples used in this study could not be readily obtained, however, since the samples were too thick for standard birefringence measurements.

It is worth noting that annealing the samples under constraints at high temperatures, irrespective of the type of stretching operation performed, always results in very low levels of shrinkage. Higher annealing temperatures were found to be necessary, however, to suppress the shrinkage of biaxially drawn samples in comparison to monoaxially drawn samples [37]. Since the orientation of the crystalline phase is not expected to be affected appreciably by the annealing treatment [38], it is reasonable to assume that the reduction in level of shrinkage brought about by annealing the samples is associated with disorientation of the chains in the amorphous phase, and that such a process is more hindered in biaxially drawn samples than in those drawn monoaxially.

It is also instructive to note that samples subjected to unbalanced biaxial stretching exhibit levels of shrinkage that are near to, and even lower than, the values recorded for the higher draw-ratio balanced biaxially oriented samples. These values are much smaller than those exhibited by the lower draw-ratio balanced biaxially oriented samples (Table I).

Correspondingly, the X-ray diffraction patterns for the unbalanced biaxially oriented samples were found to display the characteristic features of "uniplanar-axial" orientation, albeit less pronounced, associated with samples taken from the shear regions of the biaxially drawn samples. This similarity in type of orientation is to be attributed to the planarity of the deformations in both situations with a directional bias for the alignment of crystals. In other words it is the directionality of the imposed stresses that determines the type of orientation assumed by the crystals and not their origin, i.e. irrespective of whether these are shear or normal stresses.

On the basis of the foregoing discussion it is apparent that the causes for the somewhat lower shrinkage exhibited by the unbalanced biaxially drawn samples, relative to the balanced biaxially oriented samples, have to be associated with the occurrence of a certain amount of in-plane shear deformation resulting from the non-uniformity of the stretching ratio in the two perpendicular directions. Related to this is the observation that the DSC traces recorded for the unevenly drawn samples displayed only a very shallow and broad exothermic peak, with a ΔH_c less than $1.0\,\mathrm{cal\,g^{-1}}$ ($4.2\,\mathrm{J\,g^{-1}}$) even at the higher drawing temperatures, e.g. 110 °C, which provides a clear confirmation for the occurrence of stress-induced crystallization phenomena in the unevenly drawn samples.

Although a quantitative assessment of the effects of shear deformations relative to axial extensions cannot be entertained with the present results, it is clear that without rotation of the axes parallel to the drawing direction there cannot be any in-plane shear but only simple shear deformations. The latter can, nevertheless, be effective in enhancing stress-induced crystallization phenomena.

Being the result of disorientation of the amorphous phase, shrinkage may or may not be accompanied by further crystallization depending on the overall degree of crystallinity that is already present.

4. Conclusions

The main conclusions that can be drawn from this work are:

1. The superimposition of in-plane shear deformations in the biaxial stretching of PET sheets enhances considerably the dimensional stability as a result of an increase in the degree of stress-induced crystallinity.
2. The predominant factor determining the post-processing shrinkage of biaxially oriented products is the extent of orientation in the amorphous phase. Shrinkage may be assisted by thermal crystallization phenomena but the latter are not a necessary condition.

Acknowledgements

The authors wish to acknowledge the financial support received from Enichem Fibre, the Ministero dell' Universita' and della Ricerca Scientific a Technologica and the Consiglio Nazionale delle Ricerche. They are also grateful to Professor V. Petraccone for useful comments.

Appendix: Definition of draw ratios and shear ratios in biaxial stretching with planar shear distortions

The axial draw ratio in the y direction is

$$\lambda_y^T = \bar{L}_f / L_o$$

where

$$\bar{L}_f = \frac{L_{f(1)} + L_{f(2)} - L_{f(0)}}{2}$$

and that in the x direction is

$$\lambda_x^T = \bar{W}_f / W_o$$

where

$$W_f = \frac{W_{f(1)} + W_{f(2)} - W_{(f(0)}}{2}$$

The area expansion ratio is

$$\lambda_A = \frac{\text{Final area}}{\text{Original area}} = \lambda_x^T \lambda_y^T$$

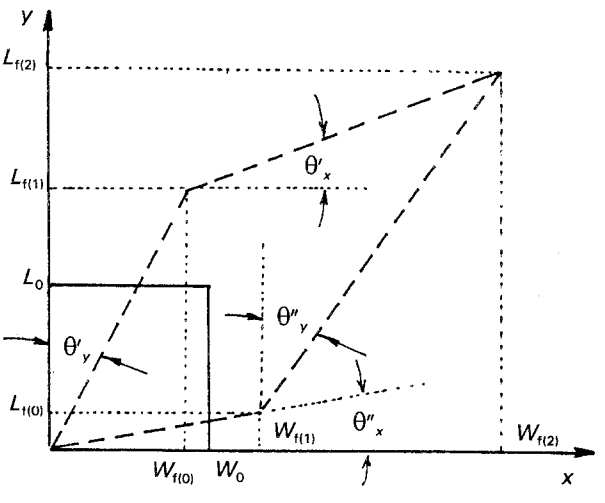

Figure A1 Biaxial stretching with planar shear.

and the average axial draw ratio is

$$\lambda_{av}^{T} = \frac{\lambda_x^T + \lambda_y^T}{2} = (\lambda_A)^{1/2}$$

The shear ratio relative to the y direction is

$$\lambda_{xy}^{S} = \sec\bar{\theta}_y = (1 + \tan^2\bar{\theta}_y)^{1/2}$$

where

$$\bar{\theta}_y = \frac{\theta'_y + \theta''_y}{2}$$

is the average angle of shear for the y direction.

The shear ratio relative to the x direction is

$$\lambda_{xy}^{S} = \sec\bar{\theta}_x = (1 + \tan^2\bar{\theta}_x)^{1/2}$$

where

$$\bar{\theta}_x = \frac{\theta'_x + \theta''_x}{2}$$

is the average angle of shear for the x direction.

References

1. "Kodapak PET, Thermoplastic Polyester" (Eastman Chemical Products Inc., Kingsport, USA, 1982).
2. W. L. CORSOEVER, Netherlands Patent 7 203 971 (1972); US Patents 3 803 275 (1974) and 3 745 150 (1973).
3. H. G. FRITZ, *Kunstoffe* **68** (1978) 450.
4. N. C. WYETH and R. N. ROSEVEORVE, US Patent 3 733 309 (1973).
5. N. H. LADIZESKY and I. M. WARD, *J. Mater. Sci.* **8** (1973) 980.
6. F. Le BOURVELLEC, L. MONNERIE and J. P. JARRY, *Polymer* **28** (1987) 1712.
7. A. J. De VRIES, C. BONNEBAT and J. BEAUTEMPS, *J. Polym. Sci., Polym. Symp.* **58** (1977) 109.
8. M. CAKMAK, J. L. WHITE and J. E. SPRUIELL, in Proceedings of ANTEC 85, 43rd Annual Technical Conference of the Society of Plastics Engineers, Washington DC, April 1985, p. 912.
9. W. J. HENNESSEY and A. L. SPATARICO, *Polym. Eng. Sci.* **19** (1979) 462.
10. P. MONARESI, P. PARRINI, G. L. SEMEGHINI and E. DEFORNASSARI, *Polymer* **17** (1976) 595.
11. G. S. Y. YEH and P. H. GEILL, *J. Macromol. Sci.* **B1** (1967) 251.
12. *Idem, ibid.* **B1** (1967) 251.
13. G. A. J. ORCHARD, P. SPIBY and I. M. WARD, *J. Polym. Sci., Polym. Phys.* **28** (1990) 603.
14. L. J. FINA, D. I. BOWER and I. M. WARD, *Polymer* **29** (1988) 2146.
15. D. A. JARVIS, I. J. HUTCHINSON, D. I. BOWER and I. M. WARD, *ibid.* **21** (1980) 41.
16. L. MASCIA and Z. FEKKAI, *ibid.* **37** (1993) 1419.
17. W. N. KIM and C. M. BURNS, *J. Appl. Polym. Sci.* **32** (1986) 2989.
18. *Idem, ibid.* **34** (1987) 945.
19. *Idem, Macromolecules* **20** (1987) 1876.
20. J. H. NOBBS, D. I. BOWER and I. M. WARD, *Polymer* **17** (1976) 25.
21. G. HINRICHSEN, H. G. ADAM, H. KREBS and H. SPRINGER, *Coll. Polym. Sci.* **285** (1980) 232.
22. V. BUSICO, P. CORRADINI, F. RIVA, A. SEVES and L. VICINI, *Makromol. Chem. Rapid Commun.* **1** (1980) 423.
23. T. SUN, J. PEREIRA and R. S. PORTER, *J. Polym. Sci., Polym., Phys., Edn* **22** (1984) 1163.
24. H. SPRINGER, U. BRINKMANN and G. HINRICHSEN, *Coll. Polym. Sci.* **259** (1981) 38.
25. M. J. NAPOLITANO and A. MOET, *J. Appl. Polym. Sci.* **34** (1987) 1285.
26. L. PARRAVICINI, B. LEONE, F. AURIEMMA, G. GUERRA, V. PETRACCONE, G. DI DINO, R. BIANCHI, R. VOSA, *J. Appl. Polym. Sci.* in press.
27. W. O. STRATTON and G. M. GODARD, *J. Appl. Phys.* **28** (1957) 1111.
28. R. P. DAUBENY, C. W. BUNN and C. BROWN, *Proc. R. Soc.* **A226** (1954) 531.
29. I. H. HALL, in "Structure of Crystalline Polymers", edited by I. H. Hall (Elsevier Applied Science, London, 1984) p. 39.
30. C. J. HEFFELFINGER and R. BURTON, *J. Polym. Sci.* **47** (1960) 289.
31. E. WENER, S. JANOKA, J. HOPPER and K. J. MacKENZIE, in "Encyclopedia of Polymer Science and Engineering", (Wiley Interscience) Vol. 12, p. 13.
32. P. CHANDRAN and S. JABARIN, *Adv. Polym. Technol.* **12** (1993) 119.
33. M. KAKUDO and N. KASAI, "X-Ray Diffraction by Polymers" (Kodansha, Tokyo, 1972) Ch. 10.
34. H. TADOKORO, "Structure of Crystalline Polymers" (Wiley, New York, 1979) p. 68.
35. M. CASEY, *Polymer* **18** (1977) 1219.
36. T. ASANO and T. SETO, *Polym. J.* **5** (1973) 72.
37. Z. FEKKAI, PhD thesis, Loughborough University of Technology (1991).
38. M. CAKMAK, J. L. WHITE, J. S. LIN and J. E. SPRUIELL, in Proceedings of ANTEC 85, 43rd Annual Technical Conference of the Society of Plastics Engineers, Washington DC, April 1985, p. 728.

Received 5 August
and accepted 8 October 1993